Is the Dispersion Relation Applicable for Exotic Nuclear Systems? The Abnormal Threshold Anomaly in the ^{6}He + ^{209}Bi System

L. Yang (杨磊), C. J. Lin (林承键),* H. M. Jia (贾会明), D. X. Wang (王东玺), N. R. Ma (马南茹), L. J. Sun (孙立杰), F. Yang (杨峰), X. X. Xu (徐新星), Z. D. Wu (吴振东), H. Q. Zhang (张焕乔), and Z. H. Liu (刘祖华)†

China Institute of Atomic Energy, P.O. Box 275(10), Beijing 102413, China

(Received 7 April 2017; revised manuscript received 24 May 2017; published 26 July 2017)

The threshold anomaly of the phenomenological potential has been known for a long time in nuclear reactions at energies around the Coulomb barrier, where the connection between the real and imaginary potentials is well described by the dispersion relation. However, this connection is not clear yet for some weakly bound nuclear systems, especially for reactions induced by exotic radioactive nuclei. In this study, precise optical potentials of the halo nuclear system ^{6}He + ^{209}Bi were extracted via ^{208}Pb(^{7}Li, ^{6}He) transfer reactions with energies measured downward to the extremely sub-barrier region. The real potential presents a bell-like shape around the barrier as a normal threshold anomaly in tightly bound nuclear systems. However, the imaginary potential shows an abnormal behavior: it increases first with energy decreasing below the barrier and then falls quickly down to 0. It is the first time the threshold of the imaginary potential has been determined in an exotic nuclear system. Moreover, experimental results show the dispersion relation is not applicable for this system, which may be a common phenomenon for exotic nuclear systems. We discuss possible explanations for such a peculiar behavior, but further study is still desired for the underlying physics.

DOI: 10.1103/PhysRevLett.119.042503

Since the optical model was first applied to describe nuclear scattering and absorptions of neutron on a variety of targets by Fernbach *et al.* [1], it has been extensively utilized with great success for the last seven decades and is now considered one of the most fundamental reaction models in nuclear physics. The essential idea is that an incident particle is scattered or absorbed when it interacts with the target [2], which is analogous to the refraction and absorption of light by a medium with complex refractive index in optics [3]. The interaction potential, namely, the optical model potential (OMP), can be written as $U(r) = V(r) + iW(r)$, where the real part describes the elastic scattering process while the imaginary part represents the absorption of incident flux, i.e., all the nonelastic reaction processes. In the mid-1980s, it was found experimentally that OMPs are energy dependent at energies around the Coulomb barrier [4,5]: the imaginary potential decreases rapidly with the effective closure of the nonelastic channels when the energy is reduced to below the barrier; hence, a threshold emerges; meanwhile, the real potential shows an anomalous variation around the barrier. This phenomenon is thus called the threshold anomaly [6–9]. For this reason, the OMP is expressed as $U(r;E) = V(r;E) + iW(r;E)$, where $V(r;E) = V_0(r;E) + \Delta V(r;E)$. The first term in the real potential arises from spatial nonlocality, usually showing a slow and smooth energy dependence over a large scale. The second term, called the dynamic polarization potential (DPP), results from the time nonlocality and links to the imaginary potential with the dispersion relation,

$$\Delta V(r;E) = \frac{P}{\pi}\int_0^\infty \frac{W(r;E)}{E'-E}\,dE', \tag{1}$$

where P is the integral principal value. The dispersion relation (known as the Kramers-Kronig relation in the general case) is a natural consequence of the causality principle, describing the effect of dispersion in a medium on the properties of a wave traveling within that medium.

The threshold anomaly is a universal phenomenon within the barrier-energy region and the dispersion relation has been confirmed by numerous experiments [6–10]. However, a distinct manifestation of the OMP is observed in reactions involving weakly bound stable nuclei ^{6}Li and ^{9}Be as well as unstable halo nuclei like ^{6}He [11–15]. In these exotic systems, the imaginary potential continuously increases with energy decreasing below the barrier. The influence of breakup reactions is considered to be the origin of this abnormal behavior [16], but the fundamental reason is yet unclear. Up to now, we are still far from a comprehensive understanding on the properties of the OMPs of exotic nuclear systems, although great progress has been achieved in the last decades [17–21]. Some long-standing puzzles are the following: Does a threshold exist in the imaginary potential? If yes, where is it? Does the dispersion relation still hold for exotic nuclear systems? To answer these questions, extremely precise OMPs are required.

In general, OMPs are extracted by fitting angular distributions of elastic scattering. However, at energies close to and below the barrier, the distributions become flat

and not enough information can be extracted. For reactions induced by unstable nuclei, the situation becomes more dire due to limitations of the intensity and/or the phase-space qualities of radioactive ion beams (RIBs). In view of this fact, a transfer reaction method [22] was proposed to study the OMPs of halo systems by the utilization of a stable beam, which can yield fairly precise results.

This method originates from a simple idea: treating the transfer reaction as the transition from the initial state $|i\rangle$ to the final state $|f\rangle$, the cross section can be written as [23]

$$(d\sigma/d\Omega)_{if} = P_{if}[(d\sigma/d\Omega)_{ii}(d\sigma/d\Omega)_{ff}]^{1/2}, \quad (2)$$

where $(d\sigma/d\Omega)_{ii}$ and $(d\sigma/d\Omega)_{ff}$ are elastic scattering cross sections in the incoming and outgoing channels, respectively. The transition probability P_{if} relates to $\langle f|V_{if}|i\rangle$, the intrinsic wave functions of the initial and final states via the interaction V_{if}, which depends on the information of nuclear structures. With the $(d\sigma/d\Omega)_{if}$ and $(d\sigma/d\Omega)_{ii}$ derived from measurements, the $(d\sigma/d\Omega)_{ff}$ can be determined with its OMP extracted by fitting the experimental data. The sensitivity of this method has been investigated theoretically [24], and the reliability was confirmed experimentally in the previous works [25,26]. In Ref. [25], an increasing trend for the imaginary potential with energy decreasing in the sub-barrier region was observed for the $^{6}\mathrm{He} + ^{209}\mathrm{Bi}$ system. However, the energy was too high to explore the threshold region, which is critical to check the dispersion relation. Therefore, more light needs to be shed on the deep sub-barrier region. With this aim, measurements at extremely low energies for the $^{208}\mathrm{Pb}(^{7}\mathrm{Li}, ^{6}\mathrm{He})^{209}\mathrm{Bi}$ transfer reaction were performed to further investigate the OMPs of $^{6}\mathrm{He} + ^{209}\mathrm{Bi}$ in the exit channel.

The experiment was carried out at the China Institute of Atomic Energy, Beijing. An isotopically enriched ^{208}Pb (99.7%) target with a thickness of about 120 μg/cm^2 on a 20 μg/cm^2 carbon backing was bombarded by a ^{7}Li beam with a typical current of about 40 pnA provided by the HI-13 tandem accelerator. Reaction energies in the laboratory frame were 21.20, 24.30, 25.67, and 28.55 MeV. Two Si-detector telescopes were fixed at the backward angle regions, with angular coverages of 99°–127° and 144°–171°, respectively. Each telescope contains three layers of Si detectors: a 20 μm single-side strip detector (16 channels) with an active area of 50×50 mm^2 as the ΔE detector and a 60 μm double-side strip detector (16×16 pixels) as well as a 1 mm quadrant silicon detector with the same areas as the residual energy (E_R) detectors. An array including eight silicon PIN-diode detectors with a coverage from 20° to 68° was mounted to measure the elastic scattering of $^{7}\mathrm{Li} + ^{208}\mathrm{Pb}$. Two additional PIN detectors were placed at ±15° as monitors, used for the data normalization since pure Rutherford scattering is expected at forward angles.

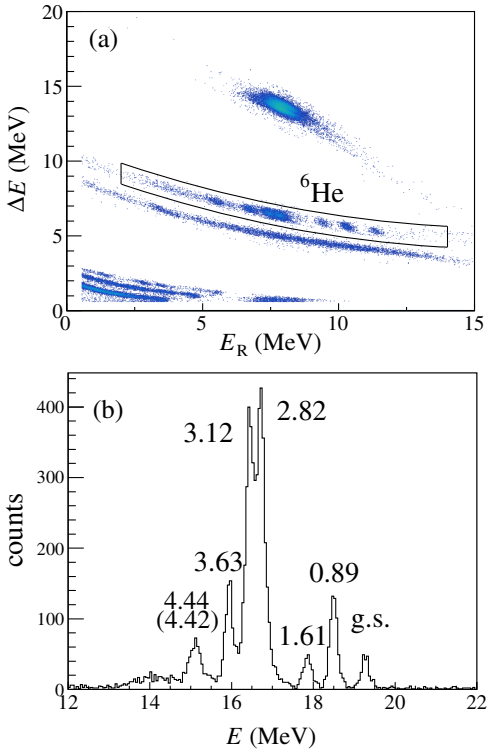

FIG. 1. $\Delta E - E_R$ spectrum (a) obtained by the telescope at $E_{\mathrm{lab}} = 28.55$ MeV with $\theta_{\mathrm{lab}} = 144° - 171°$, and the projected energy spectrum (b) of the selected ^{6}He band, where the peaks are labeled corresponding to the excitation energies of ^{209}Bi, in the unit of MeV.

The ΔE-E_R spectrum obtained by one of the telescopes at $E_{\mathrm{lab}} = 28.55$ MeV is shown in Fig. 1(a). Several energy groups inside the ^{6}He band can be observed, corresponding to one proton transferred from ^{7}Li to different single-particle states of ^{209}Bi, with excitation energies as labeled in Fig. 1(b) by projecting the total energy. Angular distributions of these transfer reactions are shown in Fig. 2(a). These final states can also be observed at $E_{\mathrm{lab}} = 25.67$ MeV, for which similar results are obtained. However, fewer final excited states can be identified as the reaction energy decreases. At the lower energies of 21.20 and 24.30 MeV, only the ground state, as well as the ground and the first excited states can be observed, respectively, as shown in Figs. 2(b) and 3. Only the statistical errors are considered for the experimental data. To extract the OMP parameters of the exit channel, the coupled reaction channels (CRC) approach was applied to fit the experimental data with the code FRESCO [27], and the fitting results are shown in Fig. 2 by the solid curves. In the calculations, postrepresentation is adopted, with the full complex remnant term considered. The full details of the analysis procedure can be found in Ref. [25]. The whole data set and the results will be published elsewhere [28].

To demonstrate the relation between the entrance and exit channels explicitly, in addition to the results of transfer

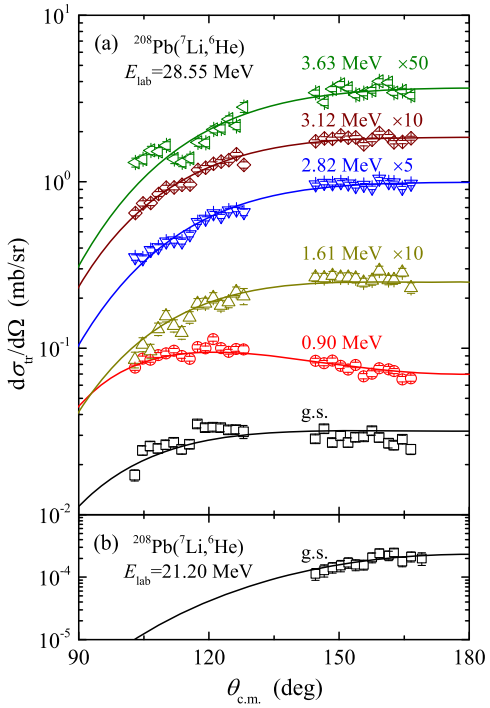

FIG. 2. Angular distributions of ^{208}Pb(^{7}Li, ^{6}He) reactions for proton transferred to different states of ^{209}Bi at $E_{lab} = 28.55$ (a) and 21.20 (b) MeV, respectively. The experimental results are labeled according to the excitation energy of ^{209}Bi. The solid curves represent the CRC fitting results.

reactions, the angular distribution of elastic scattering of ^{7}Li + ^{208}Pb at $E_{lab} = 24.30$ MeV and that of outgoing system ^{6}He + ^{209}Bi [29] at the corresponding energy ($E_{lab} = 17.84$ MeV) are also shown in Fig. 3. The solid and dotted curves show the CRC fitting results for the

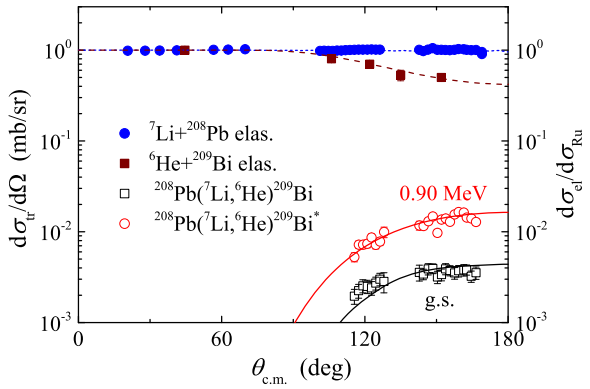

FIG. 3. Same as Fig. 2, but for $E_{lab} = 24.30$ MeV. The elastic scattering of the entrance channel ^{7}Li + ^{208}Pb as well as that of the corresponding exit channel ^{6}He + ^{209}Bi at $E_{lab} = 17.84$ MeV taken from Ref. [29] are also shown by the solid circles and squares, respectively. The dotted curve is the CRC fitting result and the dashed curve represents the calculation result with the OMP extracted from the transfer reaction.

transfer and entrance channels, respectively. It can be seen that the angular distribution for elastic scattering of the entrance channel becomes completely flat, and the transfer reactions show features of a backward focused distribution at such a deep sub-barrier energy, where the nuclear potential is very weak and becomes insensitive to the angular distribution. However, the cross section of the transfer reaction places additional constraints on the OMP parameters. Therefore, a precise OMP of the exit channel can be extracted, with the reliability confirmed by reproducing the elastic scattering of ^{6}He + ^{209}Bi properly, as the dashed curve shown in Fig. 3.

Together with our previous results at energies of 32.55, 37.55, and 42.55 MeV [25], the energy dependencies of the real and imaginary potentials at the sensitivity radius 13.5 fm are shown in Fig. 4. The errors were derived by χ^2 analysis with a confidence level of 68.3%. As shown in Fig. 4, a strong energy dependence is observed for both the real and imaginary potentials.

For the real part, a bell-like shape with maximum around the Coulomb barrier ($V_B \approx 20$ MeV in the center of mass system) is present as shown in the inset of Fig. 4(a). This behavior is similar to the normal threshold anomaly in tightly bound nuclear systems, demonstrating a large

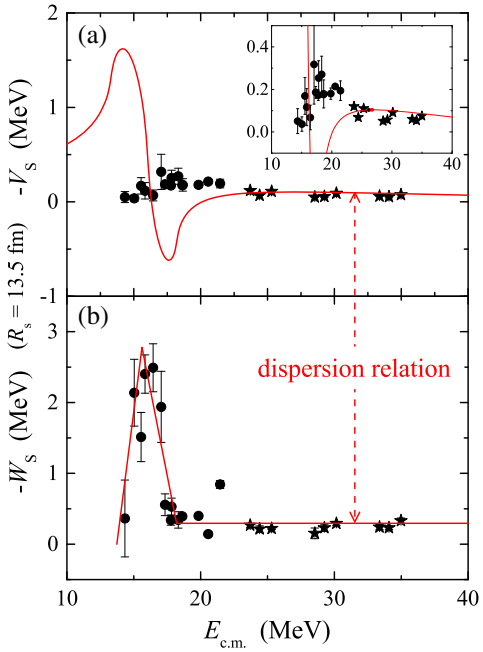

FIG. 4. Energy dependence of the real (a) and imaginary (b) potentials at the sensitivity radius of 13.5 fm for the ^{6}He + ^{209}Bi system. The present results are shown by the circles, and stars represent the previous results taken from Ref. [25]. The solid curve in (b) shows the linear segment fitting for the imaginary potential. The prediction of the dispersion relation according to the variation of the imaginary potential is present in (a) by the solid curve. The fine structure of the real potential is shown in the inset of (a).

attractive polarization effect. It may reduce the fusion barrier and result in an increased fusion probability in the sub-barrier energy region. This has been confirmed by the previous experimental data [30], where a large fusion enhancement at sub-barrier energy was observed. It is worth noting that this attractive DPP may arise from the extended matter distribution [30] and/or the soft dipole resonance [31] of ^{6}He, rather than the breakup process [32].

For the imaginary part, the strength increases first as the reaction energy decreases in the sub-barrier region. However, it is dubious to say that the increasing behavior is due to the breakup, since the transfer reaction mechanism may dominate at sub-barrier energies [30,33]. As the energy reduces further, a decreasing trend is observed clearly, vanishing at the energy of 13.73 ± 1.63 MeV (with confidence interval of 90%), according to the extrapolation. This is the threshold of the imaginary potential, at about $0.68V_B$. It is the first time that this threshold is determined for an exotic nuclear system. At the threshold energy, the distance of closest approach in the Coulomb field for a head-on collision is about $17.41^{+2.35}_{-1.85}$ fm, in good agreement with the critical interaction distance (18.91 ± 1.24 fm) extracted from the elastic backscattering data [34]. Larger than this distance, the whole system becomes inert. Compared with the threshold values of $0.93V_B$ in the tightly bound $^{16}\mathrm{O} + {}^{208}\mathrm{Pb}$ system [6] and $0.81V_B$ in the weakly bound $^6\mathrm{Li} + {}^{144}\mathrm{Sm}$ system [35] (so far, no results have been reported for ^{6}Li interacting with a heavy target), such a low threshold energy is a quite consistent feature of the extended matter distribution and minuscule binding energy of the halo nucleus ^{6}He.

Moreover, the applicability of the dispersion relation in this halo system was investigated. The calculation result for the real potential according to the dispersion relation with the variation of the imaginary part is shown by the solid curve in Fig. 4(a), where the linear schematic model [7] was employed to fit the imaginary potential as the solid line shown in Fig. 4(b). One can see that at the sub-barrier energy region, the dispersion relation predicts a repulsive DPP followed by a stronger attractive one as the energy decreases further. Comparing with the experimental results, it is clear that the dispersion relation does not hold for $^6\mathrm{He} + {}^{209}\mathrm{Bi}$, which may be a common phenomenon for exotic nuclear systems [7,36–38]. Although some references [15,39] report that the dispersion relation works well for halo nuclear systems, due to the lack of a complete picture of the imaginary potential, a large uncertainty is introduced to the dispersion relation calculations [15]. Furthermore, in a wider context the dispersion relation has to be used with extreme caution for peculiar systems, such as systems consisting of negative-refractive-index material [40].

The dispersion relation is based on the causality principle as expressed in the Kramers-Kronig relation, which is derived from Cauchy's residue theorem. To do that, some conditions have to be satisfied, one of which is that the complex plane should contain a finite list of isolated singularities, corresponding to the discrete states of the interacting nuclear system [7]. In the case of an exotic nuclear system, there exist continuum states due to the breakup process, which is in conflict with the requirement of the residue theorem. Therefore, it is not mathematically rigorous to apply the dispersion relation directly to the exotic nuclear system. It is imperative to develop a new relation to describe the abnormal behavior between the real and imaginary potentials for the exotic nuclear system where continuum states are present.

On the other hand, it is noteworthy that the phenomenological OMP extracted from experimental data is a local potential, rather than the generalized nonlocal optical potential [41]. When such a local potential is employed directly to solve the Schrödinger equation with the scattering amplitude averaged on a suitable energy interval, an additional energy dependence (the spurious energy dependence [36]) is introduced. Obviously, this spurious energy dependence arising from the spatial nonlocality effect does not follow the dispersion relation from the time nonlocality effect. Furthermore, it could be more significant when the nonlocality is of the order of magnitude of the incident wavelength [41].

In addition, the phenomenological OMP is only sensitive within a certain region, i.e., the sensitive radius located in the external part of the potential. Information about the potential in the interior region cannot be extracted experimentally [42]. Conversely, the causality principle, hence the dispersion relation, has been derived only for the potential that can yield the wave function over all spatial regions. Therefore the phenomenological potential does not necessarily need to abide by the causality property [36].

In summary, angular distributions of the transfer reaction $^{208}\mathrm{Pb}(^7\mathrm{Li}, ^6\mathrm{He})^{209}\mathrm{Bi}$ were measured at near- and sub-barrier energies. The OMP parameters of the halo system $^6\mathrm{He} + {}^{209}\mathrm{Bi}$ were extracted by fitting the experimental data within the CRC framework. A strong energy dependence was observed in both the real and imaginary potentials: the real part presents a bell-like shape around the Coulomb barrier, while for the imaginary potential, the strength increases first as the energy decreases, followed by a rapid decreasing trend as the energy becomes lower in the deep sub-barrier region. For the first time, the threshold of the imaginary potential is determined for an exotic nuclear system. Moreover, the classical dispersion relation cannot be adopted to describe the connection between the real and imaginary parts. We discussed some possible reasons for such peculiar behavior, but further study is required to discover the underlying physics. The transfer reaction method is a possible reasonable approach, not necessarily the unique one, to investigate the nuclear potential in the sub-barrier region, which is difficult (nearly impossible) to be searched with the low intensity RIBs directly. It would

be desirable to further apply this method to investigate the OMPs in a wide range of unstable nuclei and to obtain a global and universal understanding on the properties of the interaction potentials of exotic nuclear systems.

We gratefully thank Ian Thompson and D. Kahl for helpful discussion. This work is supported by the National Key Basic Research Program of China (Grant No. 2013CB834404) and by the National Natural Science Foundation of China (Grants No. 11505293, No. 11635015, No. 11375268, No. 11475263, No. U1432246, and No. U1432127).

*Corresponding author.
cjlin@ciae.ac.cn
†Deceased.

[1] S. Fernbach, R. Serber, and T. B. Taylor, Phys. Rev. **75**, 1352 (1949).
[2] H. Feshbach, Annu. Rev. Nucl. Sci. **8**, 49 (1958).
[3] P. E. Hodgson, Rep. Prog. Phys. **34**, 765 (1971).
[4] A. Baeza, B. Bilwes, R. Bilwes, J. Díaz, and J. L. Ferrero, Nucl. Phys. **A419**, 412 (1984).
[5] J. S. Lilley, B. R. Fulton, M. A. Nagarajan, I. J. Thompson, and D. W. Banes, Phys. Lett. **151B**, 181 (1985).
[6] M. A. Nagarajan, C. C. Mahaux, and G. R. Satchler, Phys. Rev. Lett. **54**, 1136 (1985).
[7] C. Mahaux, H. Ngô, and G. R. Satchler, Nucl. Phys. **A449**, 354 (1986).
[8] G. R. Satchler, Phys. Rep. **199**, 147 (1991).
[9] M. E. Brandan and G. R. Satchler, Phys. Rep. **285**, 143 (1997).
[10] C. J. Lin, J. C. Xu, H. Q. Zhang, Z. H. Liu, F. Yang, and L. X. Lu, Phys. Rev. C **63**, 064606 (2001).
[11] N. Keeley, S. J. Bennett, N. M. Clarke, B. R. Fulton, G. Tungate, P. V. Drumm, M. A. Nagarajan, and J. S. Lilley, Nucl. Phys. **A571**, 326 (1994).
[12] Zhang Chun-Lei, Zhang Huan-Qiao, Lin Cheng-Jian *et al.*, Chin. Phys. Lett. **23**, 1146 (2006).
[13] C. Signorini, A. Andrighetto, M. Ruan *et al.*, Phys. Rev. C **61**, 061603(R) (2000).
[14] N. Yu, H. Q. Zhang, H. M. Jia, S. T. Zhang, M. Ruan, F. Yang, Z. D. Wu, X. X. Xu, and C. L. Bai, J. Phys. G **37**, 075108 (2010).
[15] A. R. Garcia, J. Lubian, I. Padron, P. R. S. Gomes, T. Lacerda, V. N. Garcia, A. Gómez Camacho, and E. F. Aguilera, Phys. Rev. C **76**, 067603 (2007).
[16] M. S. Hussein, P. R. S. Gomes, J. Lubian, and L. C. Chamon, Phys. Rev. C **73**, 044610 (2006).
[17] L. F. Canto, P. R. S. Gomes, R. Donangelo, and M. S. Hussein, Phys. Rep. **424**, 1 (2006).
[18] N. Keeley, R. Raabe, N. Alamanos, and J. L. Sida, Prog. Part. Nucl. Phys. **59**, 579 (2007).
[19] N. Keeley, N. Alamanos, K. W. Kemper, and K. Rusek, Prog. Part. Nucl. Phys. **63**, 396 (2009).
[20] B. B. Back, H. Esbensen, C. L. Jiang, and K. E. Rehm, Rev. Mod. Phys. **86**, 317 (2014).
[21] L. F. Canto, P. R. S. Gomes, R. Donangelo, J. Lubian, and M. S. Hussein, Phys. Rep. **596**, 1 (2015).
[22] C. J. Lin, F. Yang, P. Zhou, H. Q. Zhang, Z. H. Liu, M. Ruan, X. K. Wu, and C. L. Zhang, AIP Conf. Proc. **853**, 81 (2006).
[23] R. Bass, *Nuclear Reactions with Heavy Ions* (Springer-Verlag, Berlin Heidelberg, 1980).
[24] Wu Zhen-Dong, Yang Lei, Lin Cheng-Jian *et al.*, Chin. Phys. Lett. **31**, 092401 (2014).
[25] L. Yang, C. J. Lin, H. M. Jia *et al.*, Phys. Rev. C **89**, 044615 (2014).
[26] L. Yang, C. J. Lin, H. M. Jia *et al.*, Phys. Rev. C **95**, 034616 (2017).
[27] I. J. Thompson, Comput. Phys. Rep. **7**, 167 (1988).
[28] L. Yang *et al.* [Phys. Rev. C (to be published)].
[29] E. F. Aguilera, J. J. Kolata, F. D. Becchetti *et al.*, Phys. Rev. C **63**, 061603(R) (2001).
[30] J. J. Kolata, V. Guimarães, D. Peterson *et al.*, Phys. Rev. Lett. **81**, 4580 (1998).
[31] S. Nakayama, T. Yamagata, H. Akimune *et al.*, Phys. Rev. Lett. **85**, 262 (2000).
[32] M. S. Hussein, L. F. Canto, and R. Donangelo, Nucl. Phys. **A722**, C321 (2003).
[33] J. J. Kolata, H. Amro, F. D. Becchetti *et al.*, Phys. Rev. C **75**, 031302(R) (2007).
[34] V. Guimarães, J. J. Kolata, E. F. Aguilera *et al.*, Phys. Rev. C **93**, 064607 (2016).
[35] J. M. Figueira, J. O. Fernández Niello, A. Arazi *et al.*, Phys. Rev. C **81**, 024613 (2010).
[36] R. Lipperheide and A. K. Schmidt, Nucl. Phys. **A112**, 65 (1968).
[37] A. Pakou, N. Alamanos, A. Lagoyannis *et al.*, Phys. Lett. B **556**, 21 (2003).
[38] A. Pakou, N. Alamanos, G. Doukelis *et al.*, Phys. Rev. C **69**, 054602 (2004).
[39] A. Gómez Camacho, E. F. Aguilera, P. R. S. Gomes, and J. Lubian, Phys. Rev. C **84**, 034615 (2011).
[40] P. Kinsler and M. W. McCall, Phys. Rev. Lett. **101**, 167401 (2008).
[41] G. Passatore, Nucl. Phys. **A95**, 694 (1967).
[42] J. G. Cramer and R. M. DeVries, Phys. Rev. C **22**, 91 (1980).